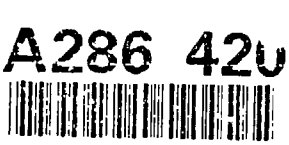

ARMY RESEARCH LABORATORY

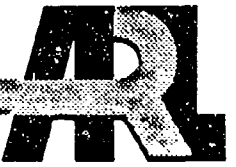

Ab Initio Potential Energy Surface for H + OCS Reactions: Extended Basis Sets and Correlation Treatment

Betsy M. Rice
Cary F. Chabalowski

ARL-TR-629 November 1994

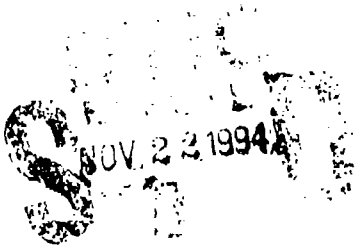

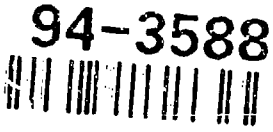

NOTICES

Destroy this report when it is no longer needed. DO NOT return it to the originator.

Additional copies of this report may be obtained from the National Technical Information Service, U.S. Department of Commerce, 5285 Port Royal Road, Springfield, VA 22161.

The findings of this report are not to be construed as an official Department of the Army position, unless so designated by other authorized documents.

The use of trade names or manufacturers' names in this report does not constitute endorsement of any commercial product

REPORT DOCUMENTATION PAGE

Form Approved
OMB No. 0704-0188

1. AGENCY USE ONLY (Leave blank)	2. REPORT DATE	3. REPORT TYPE AND DATES COVERED
	November 1994	Final, September 1993–June 1994

4. TITLE AND SUBTITLE

Ab Initio Potential Energy Surface for H + OCS Reactions: Extended Basis Sets and Correlation Treatment

5. FUNDING NUMBERS

PR: 1L161102AH43

6. AUTHOR(S)

Betsy M. Rice and Cary F. Chabalowski

7. PERFORMING ORGANIZATION NAME(S) AND ADDRESS(ES)

U.S. Army Research Laboratory
ATTN: AMSRL-WT-PC
Aberdeen Proving Ground, MD 21005-5066

8. PERFORMING ORGANIZATION REPORT NUMBER

9. SPONSORING/MONITORING AGENCY NAME(S) AND ADDRESS(ES)

U.S. Army Research Laboratory
ATTN: AMSRL-OP-AP-L
Aberdeen Proving Ground, MD 21005-5066

10. SPONSORING/MONITORING AGENCY REPORT NUMBER

ARL-TR-629

11. SUPPLEMENTARY NOTES

12a. DISTRIBUTION/AVAILABILITY STATEMENT

Approved for public release; distribution is unlimited.

12b. DISTRIBUTION CODE

13. ABSTRACT *(Maximum 200 words)*

Ab initio calculations using extended basis sets are presented for the potential energy surface (PES) of H + OCS. There are two major reaction channels on the PES; Reaction (I) is $H(^2S) + OCS(^1\Sigma) \rightarrow OH(^2\Pi) + CS(^1\Sigma)$, and Reaction (II) is $H(^2S) + OCS(^1\Sigma) \rightarrow SH(^2\Pi) + CO(^1\Sigma)$. Results of this study substantiate findings from an earlier quantum chemical study using a lower level of theory, including (1) the existence of 12 transition states and 6 stable 4-body intermediates; (2) the qualitative description of the PES (i.e., geometries, relative barriers, and well depths are similar to those in the earlier study); and (3) the entrance channel transition states leading to (II) are tight, as suggested by experiment. The results presented here also support the explanations of observed product energy distributions for (I) and (II) based on the earlier *ab initio* study. An additional transition state connecting the *cis*-HOCS and *cis*-HSCO minima was located, confirming a previous suggestion that Reaction (II) could result from hydrogen migration after HOCS formation. The current results show a substantial improvement in the quantitative agreement with experiment over the previously calculated values.

14. SUBJECT TERMS

potential energy surface, *ab initio*, MP4, QCISD(T), electronic structure, potential energy, quantum chemistry

15. NUMBER OF PAGES

33

16. PRICE CODE

17. SECURITY CLASSIFICATION OF REPORT	18. SECURITY CLASSIFICATION OF THIS PAGE	19. SECURITY CLASSIFICATION OF ABSTRACT	20. LIMITATION OF ABSTRACT
UNCLASSIFIED	UNCLASSIFIED	UNCLASSIFIED	SAR

INTENTIONALLY LEFT BLANK.

ACKNOWLEDGMENT

The authors thank Dr. H. E. Cartland and Professor C. Wittig for stimulating and encouraging conversations regarding this interesting system.

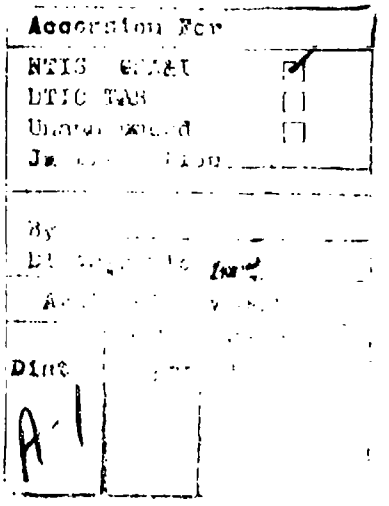

INTENTIONALLY LEFT BLANK.

TABLE OF CONTENTS

INTENTIONALLY LEFT BLANK.

LIST OF FIGURES

LIST OF TABLES

INTENTIONALLY LEFT BLANK.

1. INTRODUCTION

The following is an extension of an earlier theoretical study of the H + OCS potential energy surface (PES) (Rice, Cartland, and Chabalowski 1993). In that study, qualitative features of the following two reaction channels were calculated at the PUMP4/UMP2/6-31G** level.

$$H(^2S) + OCS(^1\Sigma) \rightarrow OH(^2\Pi) + CS(^1\Sigma) \qquad \Delta H^0_{298} = 57.2 \text{ kcal/mol} \qquad (I)$$

$$H(^2S) + OCS(^1\Sigma) \rightarrow SH(^2\Pi) + CO(^1\Sigma) \qquad \Delta H^0_{298} = -12.1 \text{ kcal/mol} \qquad (II)$$

In this study, we attempt a more quantitative prediction for the critical points on this surface. The calculations presented here use basis sets as large as Dunning's aug-cc-pVTZ (Dunning 1989; Kendall, Dunning, and Harrison 1992; Woon and Dunning 1993) and correlation corrections as high as PUMP4 and QCISD(T) (Pople, Head-Gordon, and Raghavachari 1987).

In the previous study (Rice, Cartland, and Chabalowski 1993), we found structures corresponding to minima and saddle points along the reaction pathways for (I) and (II). These consisted of 6 stable 4-body complexes and 12 saddle points, enabling us to characterize the primary reaction paths for (I) and (II). The study showed that the low-energy approach of the hydrogen to OCS is broadside, rather than end-on for both reactions. The study substantiated experimental hypotheses of the existence of stable four-body reaction intermediates (Böhmer, Mikhaylichenko, and Wittig 1993; Nickolaisen and Cartland 1993; Häusler, Rice, and Wittig 1987), and the "tight" four-body transition states leading to the products of (II) (Tsunashima et al. 1975; Lee, Stief, and Timmons 1977). Additionally, we offered qualitative explanations for the observed nonstatistical product energies distributions for Reaction (II) and the statistical product energy distributions for Reaction (I) (Böhmer, Mikhaylichenko, and Wittig 1993; Nickolaisen and Cartland 1993; Häusler, Rice, and Wittig 1987). The results of the work presented here do not change those explanations or conclusions. Unfortunately, the level of theory and basis set used in our previous study prevented us from making quantitative comparison of energetics with measured activation energies for Reaction II (Tsunashima et al. 1975; Lee, Stief, and Timmons 1977).

The thermal rate measurements of Tsunashima et al. (1975) and Lee, Stief, and Timmons (1977) provided Arrhenius parameters for Reaction (II). The activation energy and pre-exponential factor reported by Tsunashima et al. (1975), for rates measured between 300 to 525 K, are 3.90 ±0.370 kcal/mol and

1.5 ±0.20 × 10^{-11} cm^3/molecule-s. Lee, Stief, and Timmons (1977) report similar Arrhenius parameters for measurements between 261 to 500 K; they give an activation energy and pre-exponential factor of 3.85 ±0.110 kcal/mol and 9.06 ±1.53 × 10^{-12} cm^3/molecule-s, respectively. The magnitudes of the reported pre-exponential factors are small compared to other hydrogen abstraction reactions, leading the experimentalists to conclude that a tight-activated complex was involved in the formation of product (Tsunashima et al. 1975; Lee, Stief, and Timmons 1977). Our previous results supported this conclusion of a tight-activated complex. Our calculations, however, had enough error in the energetics that the activation energy issue could not be addressed.

We present results of extended basis set calculations at various levels of correlation correction for stationary points on the H + OCS PES. The purpose of this study is to provide a quantitative comparison of these energies to the experimental results, and to substantiate the existence and structure of the critical points located in the earlier study (Rice, Cartland, and Chabalowski 1993). We have also attempted to assess the accuracy of these calculations in the comparison with experimental data. As the quality of the theoretical treatment improves, a trend in the predicted energies emerges that shows convergence toward the experimental values. This allows for a rough estimate of the uncertainty in the energies calculated for the structures on the PES.

A question we did not address in the previous study was the role of hydrogen migration in the reactions. Besides locating each stationary point that was found in our previous study at the lower level of theory and basis set, we have located the transition state for the hydrogen-migration reaction. The size of this barrier, however, makes this a high-energy reaction.

2. METHODS

The calculations presented here were performed using the Gaussian 92 set of codes (Frisch et al. 1992). All geometry optimizations meet or exceed the default values for convergence in these codes. No attempts were made to correct for basis set superposition error (BSSE) (Boys and Bernardi 1970; Andzelm, Klobukowski, and Radzio-Andzelm 1984) since studies at the SCF level on the interaction energy of HF + HF for 34 different basis sets (Schwenke and Truhlar 1985, 1986) showed that the counterpoise method (Boys and Bernardi 1970), or variations of this method, gave a corrected energy that "was no more reliably accurate than the uncorrected energy" (Davidson and Feller 1986). MP calculations

reported here were run without any frozen core orbitals, while the QCISD and QCISD(T) used a set of frozen inner shell MOs. All the virtual orbitals were included for all the correlation calculations.

In the previous study, stationary points on the H + OCS ground-state PES were first located at the ROHF level (Amos and Rice 1992) using the 6-31G** basis (Hehre, Ditchfield, and Pople 1972; Hariharan and Pople 1973; Gordon 1980). Similar structures were then located for each critical point at the correlated MP2 (Møller and Plesset 1934) levels using UHF orbitals (UMP2) as the zeroth-order wavefunctions. One additional structure (structure [i] in Figure 1 of Rice, Cartland, and Chabalowski [1993]) was found at the MP2 but not at the ROHF level. Projected UMP4 energies were calculated for each stationary point located at the ROHF and UMP2 levels. UMP2 is applicable to systems well represented by the UHF determinant (Simandiras et al. 1988). Using spin contamination as a metric, all but one point calculated with the 6-31G** basis show unprojected UHF values of the spin operator S^2 to be 0.85 or less, the exception being structure [t] in Figure 1 of Rice, Cartland, and Chabalowski (1993), which has $S^2 = 0.90$. This suggests that the UHF/6-31G** wavefunctions are reasonable zeroth-order approximations to the wavefunctions.

In this study, the UMP2 optimizations were rerun for each critical point located in the previous study using the 6-311+G(2df,2p) basis set (Krishnan et al. 1980; McLean and Chandler 1980). Starting geometries for the optimizations were the UMP2/6-31G** structures. All the structures located at the UMP2/6-31G** level exist at the UMP2/6-311+G(2df,2p) level and are shown in Figure 1. In addition, a transition state connecting the *cis*-HSCO and *cis*-HOCS minima was located (structure [v], Figure 1). Harmonic vibrational frequencies were calculated for each stationary point, providing the zero-point energies and characterizing each extremum. UHF spin operators and zero-point energies are shown in Table 1. As in the previous study (Rice, Cartland, and Chabalowski 1993), the structure with the largest S^2 value of 0.89 corresponds to structure [t] in Figure 1. The UMP2/6-311+G(2df,2p) structures were treated with higher level correlation techniques including full fourth-order (SDTQ) PUMP4 (Krishnan and Pople 1978; Krishnan, Frisch, and Pople 1980) and QCISD(T) (Pople, Head-Gordon, and Raghavachari 1987) to generate single-point energies for all points on the PES. These PUMP4 and QCISD(T) results will be called "refined energies." The QCISD(T)/UMP2/6-311+G(2df,2p) results are probably the highest quality calculations for which all the points on the PES have been studied and will be called the "reference set." Absolute energies for the optimized structures are given in Table 2. The energies of these structures relative to the reactants are listed in Table 3 and illustrated in Figure 2.

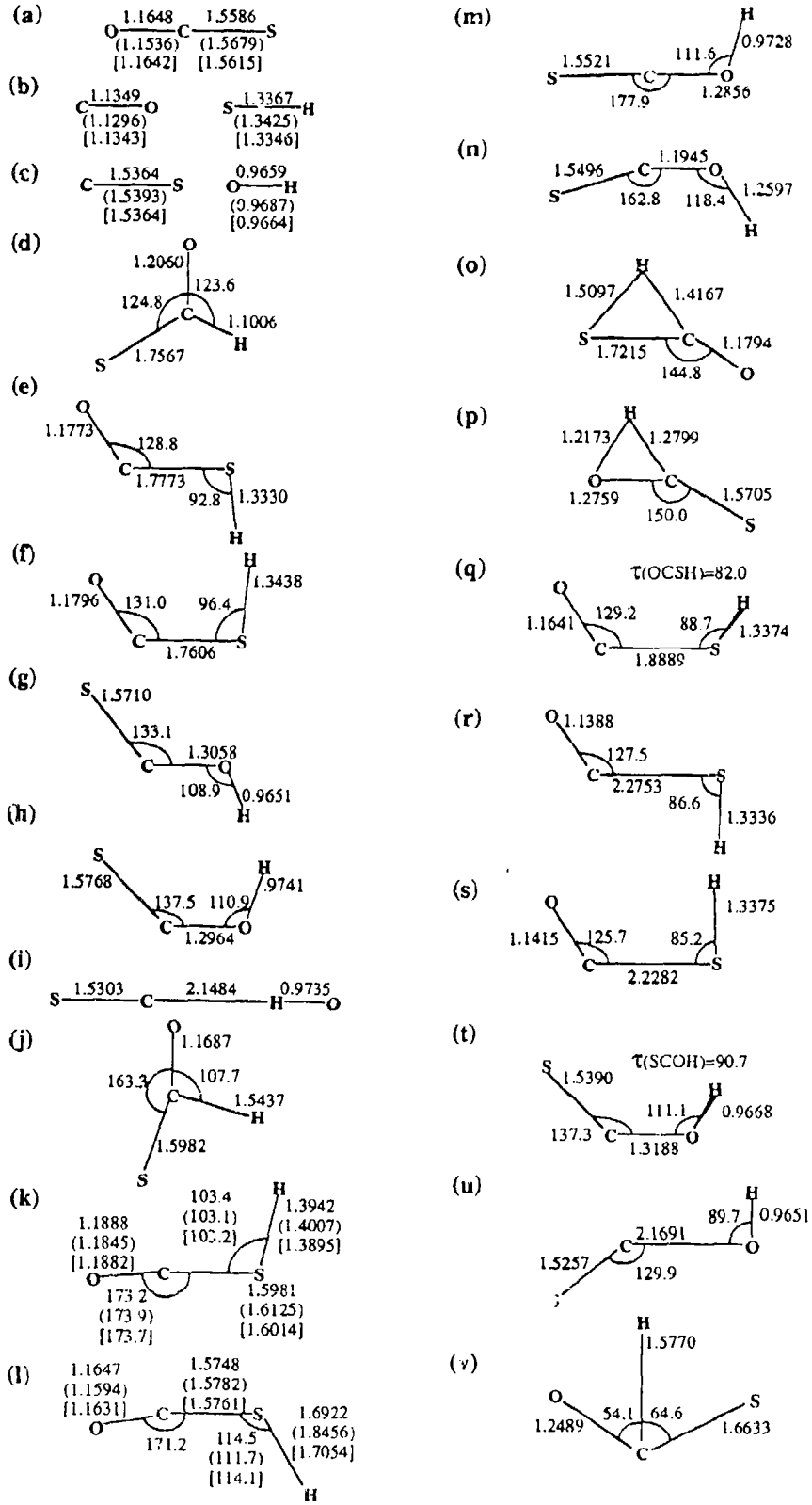

Figure 1. Optimized structures and geometric parameters at the UMP2/6-311+G(2df,2p) level. The values of the geometric parameters of structures optimized at the QCISD/6-311+G(2df,2p) and UMP2/aug-cc-pVTZ levels are given in round and square brackets, respectively.

Table 1. Zero-Point Energies (kcal/mol) and S^2 of Species on the H + OCS PES

Species		Zero-Point Energies (kcal/mol)				S^2		
		Expt.[a]	UMP2/ 6-311+G (2df,2p)	QCISD/ 6-311+G (2df,2p)	UMP2/ aug-cc-pVTZ	UMP2/ 6-311+G (2df,2p)	QCISD/ 6-311+G (2df,2p)	UMP2/ aug-cc-pVTZ
a.	H + OCS	5.66	5.84	5.84	5.79			
b.	SH + CO	6.98	6.96	6.96	7.02	0.76	0.76	0.76
c.	OH + CS	7.18	7.34	7.24	7.33	0.76	0.76	0.76
d.	HCOS		11.56			0.76		
e.	*trans*-HSCO		10.01			0.77		
f.	*cis*-HSCO		9.73			0.77		
g.	*trans*-HOCS		12.40			0.80		
h.	*cis*-HOCS		12.12			0.80		
i.	OH--CS		9.06			0.76		
j.	H + OCS → HCOS		6.93			0.82		
k.	H + OCS → *trans*-HSCO		8.81	8.68	8.87	0.78	0.78	0.78
l.	H + OCS → *cis*-HSCO		6.38	6.18	6.32	0.85	0.84	0.85
m.	H + OCS → *trans*-HOCS		11.16			0.79		
n.	H + OCS → *cis*-HOCS		7.14			0.84		
o.	HCOS → *trans* HSCO		7.84			0.79		
p.	HCOS → *trans*-HOCS		8.52			0.80		
q.	*trans*-HSCO → *cis*-HSCO		9.04			0.79		
r.	*trans*-HSCO → SH + CO		8.47			0.81		
s.	*cis*-HSCO → SH + CO		8.23			0.81		
t.	*trans*-HOCS → *cis*-HOCS		11.24			0.89		
u.	*trans*-HOCS → OH--CS		8.93			0.84		
v.	*cis*-HOCS → *cis*-HSCO		7.87			0.76		

[a] Herzberg (1945).

Table 2. Total Energies (hartrees) of Species on the H + OCS PES

Species	PUMP2/	PUMP4/	QCISD/	QCISD(T)/	QCISD/	QCISD(T)/	PUMP2/	PUMP4/	QCISD/	QCISD(T)/
	6-311+G(2df,2p)				6-311+G(2df,2p)		aug-cc-pVTZ			
	//UMP2/6-311+G(2df,2p)				//QCISD/6-311+G(2df,2p)		//UMP2/aug-cc-pVTZ			
a. H + OCS	−511.548155	−511.592798	−511.377668	−511.407010	−511.377948	−511.407014	−511.465246	−511.510336	−511.400103	−511.431250
b. SH + CO	−511.550416	−511.604573	−511.404406	−511.425688	−511.404484	−511.425656	−511.470598	−511.524983	−511.43[illegible]	−511.454343
c. OH + CS	−511.435551	−511.495157	−511.292468	−511.316903	−511.296925	−511.316975	−511.353300	−511.412897	−511.318876	−511.345153
d. HCOS	−511.558583	−511.608954	−511.404478	−511.429002						
e. *trans*-HSCO	−511.560451	−511.610693	−511.403744	−511.429600						
f. *cis*-HSCO	−511.556047	−511.606535	−511.400185	−511.425848						
g. *trans*-HOCS	−511.540447	−511.588969	−511.382732	−511.409241						
h. *cis*-HOCS	−511.538556	−511.587037	−511.381505	−511.407862						
i. OH--CS	−511.444339	−511.503452	−511.299550	−511.324461						
j. H + OCS → HCOS	−511.529324	−511.577572	−511.392717	−511.392555						
k. H + OCS → *trans*-HSCO	−511.527652	−511.577257	−511.369344	−511.395648	−511.369533	−511.395812	−511.448938	−511.499117	−511.394582	−511.422544
l. H + OCS → *cis*-HSCO	−511.533991	−511.581908	−511.368022	−511.397040	−511.366496	−511.396236	−511.453960	−511.502226	−511.391946	−511.423012
m. H + OCS → *trans*-HOCS	−511.508304	−511.556447	−511.350406	−511.376058						
n. H + OCS → *cis*-HOCS	−511.504160	−511.551143	−511.339383	−511.369042						
o. HCOS → *trans*-HSCO	−511.510252	−511.559073	−511.346215	−511.375903						
p. HCOS → *trans*-HOCS	−511.483918	−511.533281	−511.321330	−511.351481						
q. *trans*-HSCO → *cis*-HSCO	−511.547183	−511.598443	−511.391524	−511.417174						
r. *trans*-HSCO → SH + CO	−511.550244	−511.603496	−511.398133	−511.422632						
s. *cis*-HSCO → SH + CO	−511.547244	−511.600372	−511.394177	−511.419156						
t. *trans*-HOCS → *cis*-HOCS	−511.520725	−511.569183	−511.365346	−511.391362						
u. *trans*-HOCS → OH--CS	−511.442190	−511.501630	−511.296632	−511.323800						
v. *cis*-HOCS → *cis*-HSCO	−511.478142	−511.526924	−511.315364	−511.345928						

Table 3. Relative Energy (kcal/mol) of Species on the H + OCS PES

Species	PUMP2/	PUMP4/	QCISD/	QCISD(T)/	QCISD/	QCISD(T)/	PUMP2/	PUMP4/	QCISD/	QCISD(T)/
	6-311+G(2df,2p)				6-311+G(2df,2p)		aug-cc-pVTZ			
	//UMP2/6-311+G(2df,2p)				//QCISD/6-311+G(2df,2p)		//UMP2/aug-cc-pVTZ			
a. H + OCS	0.0	0.0	0.0	0.0	0.0	0.0	0.0	0.0	0.0	0.0
b. SH + CO	−1.4	7.4	−19.8	−11.7	−16.7	−11.7	−3.4	−9.2	−19.6	−14.5
c. OH + CS	70.7	61.3	53.5	56.5	50.8	56.5	70.2	61.1	51.0	54.0
d. HCOS	−6.5	−10.1	−16.8	−13.8						
e. *trans*-HSCO	−7.7	−11.2	−16.4	−14.2						
f. *cis*-HSCO	−5.0	−8.6	−14.1	−11.8						
g. *trans*-HOCS	4.8	2.4	−3.2	−1.4						
h. *cis*-HOCS	6.0	3.6	−2.4	−0.5						
i. OH–CS	65.2	56.1	49.0	51.8						
j. H + OCS → HCOS	11.8	9.6	9.4	9.1						
k. H + OCS → *trans*-HSCO	12.9	9.8	5.2	7.1	5.3	7.0	10.2	7.0	3.5	5.3
l. H + OCS → *cis*-HSCO	8.9	6.8	6.1	6.3	7.2	6.8	7.1	5.1	5.1	5.2
m. H + OCS → *trans*-HOCS	25.0	22.8	17.1	19.4						
n. H + OCS → *cis*-HOCS	27.6	26.1	24.0	23.8						
o. HCOS → *trans*-HSCO	23.8	21.2	19.7	19.5						
p. HCOS → *trans*-HOSC	40.3	37.4	35.4	34.8						
q. *trans*-HSCO → *cis*-HSCO	0.6	−3.5	−8.7	−6.4						
r. *trans*-HSCO → SH + CO	−1.3	−6.7	−12.8	−9.8						
s. *cis*-HSCO → SH + CO	0.6	−4.8	−10.4	−7.6						
t. *trans*-HOCS → *cis*-HOCS	17.2	14.8	7.7	9.8						
u. *trans*-HOCS → OH–CS	66.5	57.2	50.9	52.2						
v. *cis*-HOCS → *cis*-HSCO	43.9	41.3	39.1	38.3						

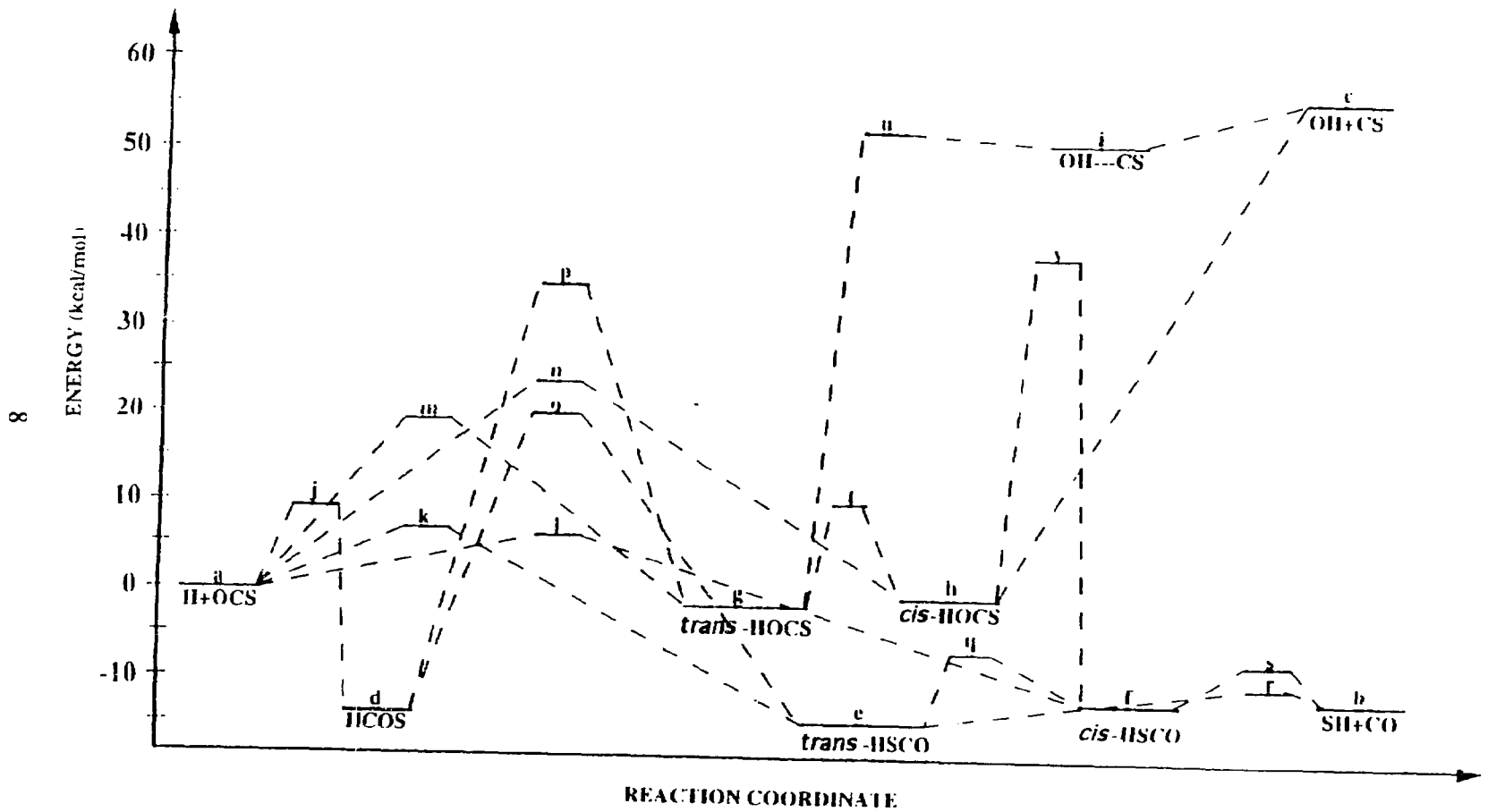

Figure 2. Energy level diagram for the H + OCS PES showing the minima and saddle-point energies at the QCISD(T)/UMP2/6-311+G(2df,2p) level.

As a further check on the basis set dependence, the reactants, products, and the two saddle-point structures labeled [k] and [l] in Figure 1 were reoptimized at the UMP2 level using Dunning's basis set aug-cc-pVTZ (Dunning 1989; Kendall, Dunning, and Harrison 1992; Woon and Dunning 1993). These structures, and the aug-cc-pVTZ basis, were then used to calculate the refined energies with full fourth-order PUMP4 and QCISD(T). Only these two saddle points (which correspond to the two entrance channel barriers to HSCO formation) were studied due to the extensive computational resources needed to do these calculations. The aug-cc-pVTZ and 6-311+G(2df,2p) basis sets differ primarily in that the former was developed to optimize correlation corrections to the energies on atoms while the latter basis was developed at the HF level. With respect to the number and types of basis functions, the sulfur, carbon, and oxygen atoms each have an additional single primitive Gaussian polarization function added at both the d- and f-orbital levels in the aug-cc-pVTZ compared to the 6-311+G(2df,2p). In addition, Dunning's hydrogen basis contains d-type polarization functions that do not exist in the other basis (Dunning 1989; Kendall, Dunning, and Harrison 1992; Woon and Dunning 1993). The valence spaces for these two basis sets have the same number of contracted AOs on hydrogen and the first-row atoms. For sulfur, the 6-311+G(2df,2p) contains one additional valence s- and p-type AO, but lacks the diffuse d- and f-type AOs. The aug-cc-pVTZ contains 165 contracted AOs for H + OCS, while the 6-311+G(2df,2p) basis has 119 AOs, with the primary difference being attributed to the extra diffuse polarization functions in the aug-cc-pVTZ basis. It might be worth pointing out that the 6-311+G(2df,2p) basis set is larger in both the valence and polarization AO spaces than the 6-311G* basis used in Pople et al.'s G1 and G2 approaches (Pople et al. 1989; Curtiss et al. 1991). Finally, to check what effect correlation has on the optimized structures, the geometries for these five points were reoptimized using QCISD/6-311+G(2df,2p), followed by an energy refinement at QCISD(T)/6-311+G(2df,2p). The results of the extended treatments with the Dunning basis set and the QCISD geometry optimizations are listed in Tables 1–4.

The knowledgeable reader might have noticed strong similarities between the current computational approach and the well-known "G1" and "G2" approaches of Pople and coworkers (Pople et al. 1989; Curtiss et al. 1991). We stress that we have not followed the G1 and G2 guidelines exactly; therefore, these are not G1-G2 type calculations. The basis sets used in our calculations contain at most a (2df) set of polarization functions for nonhydrogenic atoms and not the (3df) set recommended in the G2 approach. This choice was forced by computational limitations. However, our structures were found at MP2 (and QCISD) using a significantly larger basis set than recommended in G1 and G2. This was done to maximize our chances for accurately calculating transition state structures with elongated bond

Table 4. Vibrational Frequencies (cm^{-1}) for Stable Points and Saddle Points Calculated at the UMP2/6-311+G(2df,2p), QCISD/6-311+G(2df,2p), and UMP2/aug-cc-pVTZ Levels

Species	Calc.	Exp[30]	Species	Calc.	Species	Calc.	Species	Calc.	Species	Calc.
a. H + OCS	540	520	g. *trans*-HOCS	457	k. H + OCS → *trans*-HSCO	714*i*	o. HCOS → *trans*-HSCO	1786*i*	s. *cis*-HSCO → H + CO	313*i*
	540	520		611		479		380		127
	897	859		1018		727		485		272
	2110	2062		1292		918		722		581
				1500		1999		1844		2053
b. SH	2736	2712		3798		2040		2052		2727
CO	2135	2170								
			h. *cis*-HOCS	455	l. H + OCS → *cis*-HSCO	1360*i*	p. HCOS → *trans*-HOCS	1798*i*	t. *trans*-HOCS → *cis*-HOCS	855*i*
c. OH	3826	3738		645		415		538		500
CS	1307	1285		975		540		554		972
				1271		567		980		1097
d. HCOS	372			1507		879		1560		1501
	703			3627		2059		2325		3796
	944									
	1363		i. OH–CS	74	m. H + OCS → *trans*-HOCS	777*i*	q. *trans*-HSCO → *cis*-HSCO	368*i*	u. *trans*-HOCS → OH–CS	286*i*
	1703			76		464		347		154
	3001			139		822		557		194
				464		1227		758		642
e. *trans*-HSCO	395			560		1726		1933		1417
	404			1339		3569		2726		3842
	632			3683						
	966									
	1851		j. H + OCS → HCOS	1366*i*	n. H + OCS → *cis*-HOCS	3282*i*	r. *trans*-HSCO → SH + CO	246*i*	v. *cis*-HOCS → *cis*-HSCO	1901*i*
	2754			590		475		179		601
				623		612		260		864
f. *cis*-HSCO	401			691		944		646		894
	420			927		947		2089		1437
	566			2018		2013		2754		1708
	910									
	1844									
	2662									

(QCISD/6-311+G(2df,2p)) and [UMP2/aug-cc-pVTZ]

a. H + OCS	(544)	[526]	b. SH	(2678)	[2775]	c. OH	(3774)	[3820]	k. H + OCS → *trans*-HSCO	
	(544)	[526]	CO	(2192)	[2136]	CS	(1291)	[1309]	(695*i*)	[723*i*]
	(875)	[894]							(470)	[466]
	(2120)	[2102]							(714)	[729]
									(906)	[921]
									(1953)	[2001]
									(2027)	[2089]

l. H + OCS → *cis*-HSCO	
(936*i*)	[1354*i*]
(342)	[396]
(515)	[528]
(532)	[559]
(852)	[877]
(2079)	[2058]

and allowing for the possibility of molecular complexes to occur. In addition, no "higher level correction" (HLC) (Pople et al. 1989; Curtiss et al. 1991) was applied.

3. RESULTS AND DISCUSSION

All critical points found in our previous study (Rice, Cartland, and Chabalowski 1993) were found in these larger calculations. Additionally, another saddle point that connects the *cis*-HOCS and *cis*-HSCO wells was located. This structure (labeled [v] in Figure 1) affirms that hydrogen migration is possible for this system, as previously suggested (Böhmer, Mikhaylichenko, and Wittig 1993; Häusler, Rice, and Wittig 1987). However, reaction through this pathway is energetically unfavored, due to the size of the migration barrier. Isomerization from *cis*-HOCS to *cis*-HSCO at the QCISD(T)/UMP2/6-311+G(2df,2p) level required 38.8 kcal/mol. For completeness, we sought and found structure [v] at the UMP2/6-31G** level used in our previous work. No attempt was made to locate structure [v] at the ROHF level.

The structures obtained from the UMP2/6-311+G(2df,2p) calculations are quite similar to those found with the smaller 6-31G** basis in our previous work (see Figure 1 of Rice, Cartland, and Chabalowski [1993]), showing a stability in structure with respect to basis set size. This convergence of structures with respect to basis set size is further substantiated by comparison of the UMP2/aug-cc-pVTZ results given in Figure 1 for structures [a], [b], [c], [k], and [l], represented by the numbers in square brackets. Comparison with the nonbracketed UMP2/6-311+G(2df,2p) values shows very little change between the bond lengths and angles calculated with these two bases. A particularly interesting fact is that the structures first located at the ROHF level (Rice, Cartland, and Chabalowski 1993) for all the critical points on the PES except structure [i] are very similar to those found at the UMP2 level for all bases considered here.

We can also compare the effect of higher order correlation on structures [a], [b], [c], [k], and [l] by looking at the values for the QCISD/6-311+G(2df,2p) angles and bond lengths (reported in round brackets in Figure 1) with the UMP2/6-311+G(2df,2p) values (unbracketed). The only significant variation is the S-H bond length in the saddle-point structure [l]. The UMP2/6-311+G(2df,2p) and UMP2/aug-cc-pVTZ calculations predict this distance to be 1.69 Å and 1.71 Å, respectively. The QCISD/6-311+G(2df,2p) value, 1.85 Å, is 8–9% longer than the UMP2 values. Apart from this S-H bond length, the structures calculated at the ROHF, UMP2, and QCISD levels are similar, suggesting there will be no gross structural changes if higher levels of correlation are used to determine geometries.

Table 3 gives a summary of the energies for all stationary points on the PES relative to the H + OCS asymptote. The values in Table 3 are uncorrected and come directly from differences in calculated total energies. The features of the PES are illustrated in Figure 2 and are very similar to the features of the PUMP4/UMP2/6-31G** PES (see Figure 2 of Rice, Cartland, and Chabalowski [1993]). The relative barrier heights and well depths of the PUMP4/UMP2/6-31G** PES (Rice, Cartland, and Chabalowski 1993) provided an explanation for the observed product energy distributions for both (I) and (II).

For Reaction (II), nonstatistical product energy distributions were observed. CO vibrational and rotational distributions and the SD rotational distributions were colder than predicted by statistical theory (Böhmer, Mikhaylichenko, and Wittig 1993; Nickolaisen and Cartland 1993; Häusler, Rice, and Wittig 1987). Nickolaisen and Cartland determined that as much as 49% of available product energy was in SH vibration (Nickolaisen and Cartland 1993). The explanation for these observations put forth in our previous study (Rice, Cartland, and Chabalowski 1993) states that upon formation of HSCO, the molecule has sufficient energy to easily go on to product, due to the sizes of the entrance and exit barriers and well depth of HSCO. Most of this excess energy will initially be localized in the nascent S-H bond and adjacent HSC bend. The small exit barrier and excess energy almost ensure that the HSCO molecule will be short-lived, decomposing before intramolecular vibrational relaxation (IVR) is complete. Incomplete IVR would result in nonstatistical product energy distributions.

The large exit channel barrier (close to the endothermicity of reaction) for Reaction (I), on the other hand, almost guarantees a long-lived HOCS complex before decomposition to product. The longer lifetime of the molecule would allow complete IVR before decomposition, resulting in a statistical distribution of product energies, as observed in experiment. The qualitative nature of the surface has not changed in this study; therefore, the rationalization of the product energy distributions for both reactions offered in our previous study (Rice, Cartland, and Chabalowski 1993) still hold.

The experimental and calculated enthalpies (corrected to T = 298 K) for Reactions (I) and (II) are given in Table 5. The theoretical numbers include zero-point energy corrections. Table 5 contains results for the two basis sets 6-311+G(2df,2p) and aug-cc-pVTZ where structure optimizations were done using either the UMP2 or QCISD levels. All the final energy refinements reported in Table 5 were done at the QCISD(T) level.

Table 5. Temperature Corrected (T = 298 K) Theoretical and Experimental Reaction Enthalpies (kcal/mol)

	Rx. (I)		Rx. (II)	
Experiment:	ΔH	Ref.	ΔH	Ref.
	45.3	a	-9.8	f
	47.1	b	-9.8	g,h
	53.42	c	-10.3 ±3.0	d
	55 ±3.1	d	-10.45	b
	57.2 ±6.0	e	-11.0	i
			-11.3	a
			-12.1 ±1.2	e
			-13	c
Theoretical:				
(1) ΔE: QCISD(T)/6-311+G(2df,2p)//UMP2/6-311+G(2df,2p) Frequencies: UMP2/6-311+G(2df,2p)	59.8		-8.8	
(2) ΔE: QCISD(T)/6-311+G(2df,2p)//QCISD/6-311+G(2df,2p) Frequencies: QCISD/6-311+G(2df,2p)	59.7		-8.8	
(3) ΔE: QCISD(T)/aug-cc-pVTZ//UMP2/aug-cc-pVTZ Frequencies: UMP2/aug-cc-pVTZ	57.3		-11.5	

[a] Nickolaisen (1991)
[b] Wagman et al. (1982)
[c] Herzberg (1945)
[d] Häusler, Rice, and Wittig (1987)
[e] Chase et al. (1985)
[f] Tsunashima et al. (1975)
[g] Oldershaw and Porter (1972)
[h] Oldershaw and Smith (1978)
[i] Lee, Stief, and Timmons (1977)

3.1 Reaction (I): H + OCS → OH + CS. Comparison of calculated and experimental enthalpies are presented in Table 5. There are three sets of calculations listed under the theoretical subheading, showing the level of theory and basis set used.

Entries (1) and (2) under the Theoretical subheading in Table 5 show that the reaction enthalpy for (I) is the same whether the geometry is optimized at the UMP2 or QCISD levels. This simply verifies that the characteristics of the products and reactant species are quite similar when determined by the two correlation methods. Entry (3) shows the effect of the larger, "correlation consistent" (Dunning 1989; Kendall, Dunning, and Harrison 1992; Woon and Dunning 1993) aug-cc-pVTZ basis set. In this calculation, ΔH decreases by 2.5 kcal/mol compared to the values calculated using the 6-311+G(2df,2p)

basis. There is a large range of values given by various experiments (45.3 to 57.2 kcal/mol) (Häusler, Rice, and Wittig 1987; Herzberg 1945; Huber and Herzberg 1979; Nickolaisen 1991; Wagman et al. 1982; Chase et al. 1985) for this reaction. It is difficult for us to unequivocally choose the "best" value from this range, but our calculations support the value of Chase et al. (1985) (57.2 ±6.0 kcal/mol). All calculated ΔH's in Table 5 fall within the experimental uncertainty of the Chase et al. (1985) value, with the QCISD(T)/aug-cc-pVTZ value agreeing most closely. Such close agreement for entry (3) is most likely fortuitous, but it does lend support to the possible quantitative nature of these calculations.

Figure 2 shows that the paths leading to formation of the products of Reaction (I) [as well as for Reaction (II)] are anything but simple. Possible direct pathways to formation of the products of (I) are:

$$H + OCS \xrightarrow{[m]} \textit{trans} - HOCS \xrightarrow{[u]} OH--CS \longrightarrow OH + CS \qquad \text{(I.A)}$$

$$H + OCS \xrightarrow{[n]} \textit{cis} - HOCS \longrightarrow OH + CS \qquad \text{(I.B)}$$

Also, some reactions involving isomerization of the four-body species that could lead to products are:

$$H + OCS \xrightarrow{[j]} HOCS \xrightarrow{[p]} \textit{trans} - HOCS \xrightarrow{[u]} OH--CS$$
$$\longrightarrow OH + CS \qquad \text{(I.C)}$$

$$H + OCS \xrightarrow{[n]} \textit{cis} - HOCS \xrightarrow{[t]} \textit{trans} - HOCS \xrightarrow{[u]} OH--CS$$
$$\longrightarrow OH + CS \qquad \text{(I.D)}$$

$$H + OCS \xrightarrow{[m]} \textit{trans} - HOCS \xrightarrow{[t]} \textit{cis} - HOCS \longrightarrow OH + CS \qquad \text{(I.E)}$$

$$H + OCS \xrightarrow{[l]} \textit{cis} - HSCO \xrightarrow{[v]} \textit{cis} - HOCS \longrightarrow OH + CS \qquad \text{(I.F)}$$

$$H + OCS \xrightarrow{[l]} cis\text{-}HSCO \xrightarrow{[v]} cis\text{-}HOCS \xrightarrow{[t]} trans\text{-}HOCS$$

$$\xrightarrow{[u]} OH\text{--}CS \longrightarrow OH + CS \qquad \text{(I.G)}$$

We did not include all isomerization reactions that involve formation of *cis*-HSCO (through formation of *trans*-HSCO either directly or through formation of HCOS); the few listed above indicate the possible pathways that can be accessed given enough energy.

Although we cannot conclude that the most probable reaction paths are (I.A) and (I.B) without doing dynamics, they are the most direct. The two entrance channel barriers, [m] and [n], for these direct paths are substantially lower (<25 kcal/mol) than the reaction endothermicity (>50 kcal/mol). The structures suggest that hydrogen prefers a side-on attack, with C-O-H angles of 118° and 112° for the *cis*- and *trans*-species, respectively. We were unable to locate, as in the previous study (Rice, Cartland, and Chabalowski 1993), an exit channel barrier leading from *cis*-HOCS to product. However, the path leading from *trans*-HOCS must overcome a barrier, [u], which lies below, but close to the endothermicity of reaction. To pass from [u] to products, the reaction goes through an interesting intermediate that is stable (with respect to [u]) by only 0.4 kcal/mol. This stable intermediate, [i], represents a linear OH--CS geometry when hydrogen has now rotated to point toward carbon at a large separation of 2.15 Å.

The barrier to formation of the HCOS species (hydrogen is attached to the central carbon atom) is less than half of those leading to direct HOCS formation. However, to go on to the product of (I), HCOS must overcome a large isomerization barrier, [p], to form *trans*-HOCS. This isomerization requires approximately 16 kcal/mol more to reach *trans*-HOCS [g] than does the direct attack of H on O. Also, the barrier to formation of *cis*-HSCO is the lowest barrier on this PES; however, the isomerization to *cis*-HOCS, necessary to go to the products of (I), is substantial (~50 kcal/mol). Since the energy of the products is greater than all barriers on this PES, all of the paths listed above are energetically accessible for reaction conditions that will lead to (I).

3.2 Reaction (II): H + OCS → SH + CO. The experimentally determined reaction enthalpies for (II) range from −9.8 to −13 kcal/mol (Häusler, Rice, and Wittig 1987; Tsunashima et al. 1975; Lee, Stief, and Timmons 1977; Herzberg 1945; Huber and Herzberg 1979; Nickolaisen 1991; Wagman et al. 1982;

Chase et al. 1985; Oldershaw and Porter 1972; Oldershaw and Smith 1978). If one assumes, as we did in our comparisons for Reaction (I), that the critically evaluated enthalpy given by Chase et al. (1985) is the most reliable number, then experimental reaction enthalpy for Reaction (II) is −12.1 ±1.2 kcal/mol. Table 5 shows that UMP2 and QCISD reaction enthalpies calculated with the 6-311+G(2df,2p) basis are predicted to be −8.8 kcal/mol, or 3.3 kcal/mol higher than the Chase et al. (1985) value and 1.0 kcal/mol above the highest reported experimental value (Tsunashima et al. 1975; Oldershaw and Porter 1972; Oldershaw and Smith 1978). However, the results from the larger "correlation consistent" basis set calculation [entry (3), Table 5] give ΔH = −11.5 kcal/mol, well within the ±1.2 kcal/mol uncertainty in the Chase et al. (1985) value. The results of ΔH calculated for Reactions (I) and (II) show that the energetics of this system are not converged with respect to basis set at the 6-311+G(2df,2p) level, but approach basis set convergence with the aug-cc-pVTZ basis, at least if one defines convergence as predicting reaction enthalpies that fall within experimental uncertainty. It must be pointed out that moving from the 6-311+G(2df,2p) to the aug-cc-pVTZ basis is accompanied with a sizable increase in computational effort. Given the range of experimental data for (II), and that the Chase et al. (1985) value is at the low end of this range, it is probably safe to say that the 3.3 kcal/mol error obtained using the 6-311+G(2df,2p) basis is an upper limit, and that the actual error is less.

The portion of the PES for Reaction (II) is, as for Reaction (I), very complex. Figure 2 shows several pathways for reaching the products SH + CO, many involving isomerizations. Some of them include:

$$H + OCS \xrightarrow{[k]} \textit{trans}\text{-}HSCO \xrightarrow{[r]} SH + CO \qquad \text{(II.A)}$$

$$H + OCS \xrightarrow{[l]} \textit{cis}\text{-}HSCO \xrightarrow{[s]} SH + CO \qquad \text{(II.B)}$$

$$H + OCS \xrightarrow{[j]} HCOS \xrightarrow{[o]} \textit{trans}\text{-}HSCO \xrightarrow{[r]} SH + CO \qquad \text{(II.C)}$$

$$H + OCS \xrightarrow{[l]} \textit{cis}\text{-}HSCO \xrightarrow{[q]} \textit{trans}\text{-}HSCO \xrightarrow{[r]} SH + CO \qquad \text{(II.D)}$$

$$H + OCS \xrightarrow{[k]} \textit{trans}\text{-}HSCO \xrightarrow{[q]} \textit{cis}\text{-}HSCO \xrightarrow{[s]} SH + CO \qquad \text{(II.E)}$$

$$H + OCS \xrightarrow{[n]} cis\text{-}HSCO \xrightarrow{[v]} cis\text{-}HSCO \xrightarrow{[s]} SH + CO \qquad \text{(II.F)}$$

As in our analysis of paths resulting in Reaction (I), we have not included all of the possible isomerization reactions (such as formation of *trans*-HOCS, then isomerization to *cis*-HOCS, etc.) in the previously mentioned list. However, they are possible under the correct experimental conditions.

Reactions (II.C) and (II.F) are high-energy paths, and probably minor contributors to the reaction. High-energy pathway (II.F), and derivatives of it, appeared with the discovery of the *cis*-HOCS to *cis*-HSCO hydrogen-migration barrier [v]. This transition state is the highest energy barrier along any of the pathways involving H-atom migration (~40 kcal/mol). Once over this barrier, the system has ample energy to proceed to SH + CO. Any paths leading to *cis*-HOCS followed by H-atom migration to the sulfur could represent the hydrogen-migration path suggested previously as a possible mechanism (Böhmer, Mikhaylichenko, and Wittig 1993; Häusler, Rice, and Wittig 1987). In the more recent of these two experimental papers (Böhmer, Mikhaylichenko, and Wittig 1993), the authors used structures and relative energies from our earlier study (Rice, Cartland, and Chabalowski 1993) to cast doubt on this path as a viable mechanism for producing the observed vibrationally cool CO product. They also argued that a sudden shortening of the elongated C-O bond in HOCS should occur (e.g., structure [h]) when H undergoes a 1,3 shift from O to S and on to products. This should produce a vibrationally excited CO stretch thus giving an energy distribution considerably hotter in the stretch mode, just the opposite to what is observed experimentally (Böhmer, Mikhaylichenko, and Wittig 1993; Häusler, Rice, and Wittig 1987). The current results further support their interpretations.

High-energy pathway (II.C) begins with H attacking the central carbon atom to form the stable HCOS intermediate [d], discussed in the previous section. From here the H-atom migrates to sulfur over the largest barrier along this path, [o]. Isomerization from HCOS to *trans*-HSCO requires ~30 kcal/mol. After crossing [o], the nascent *trans*-HSCO will have sufficient excess energy to easily go onto products.

One of the more interesting results from this work comes from calculations of the barriers for the two low-energy pathways for (II) at higher levels of theory. The pathways involve direct attack of the H atom on the sulfur. In the previous study (Rice, Cartland, and Chabalowski 1993), the lowest entrance channel

barrier for this reaction was formation of *cis*-HSCO (12 kcal/mol); the next higher barrier (formation of *trans*-HSCO) was 3 kcal/mol higher. This energy separation between the two barriers showed that the major contribution to the thermal rate would be due to reaction via the *cis*-HSCO formation. In this study, however, the barrier to formation of *trans*-HSCO is more strongly influenced with the increase in correlation and basis set. The barriers {[k] (*trans*-HSCO) and [[l] (*cis*-HSCO)} have calculated heights of 7.1 kcal/mol and 6.3 kcal/mol at the QCISD(T)//UMP2/6-311+G(2df,2p) level, respectively. As seen in Figure 2, once the entrance barriers [k] and [l] are overcome, the molecules have enough excess energy to overcome the exit barriers [r] and [s] (*trans*- and *cis*-, respectively) and go on to products, making the entrance channel barriers the rate limiting step along each reaction path.

Having alluded to the probable uncertainties (supra vide) in the present calculations, the energy difference of 0.8 kcal/mol between these two barriers is too small to make any strong statement about the relative ordering of the two barriers. We carried out a series of calculations for these two entrance channel barriers, in an attempt to quantify our results. The barrier heights for [k] and [l], respectively, are 7.0 kcal/mol and 6.8 kcal/mol at the QCISD(T)//QCISD/6-311+G(2df,2p) level, and 5.3 kcal/mol and 5.2 kcal/mol at the QCISD(T)//UMP2/aug-cc-pVTZ level. From what we consider our best calculations (QCISD(T)//UMP2/aug-cc-pVTZ), the entrance channel barrier to formation of *cis*-HSCO lies only 0.10 kcal/mol below the barrier to formation of *trans*-HSCO.

One notable exception to energetic ordering of barriers to formation of *cis*- and *trans*-HSCO occurs in the QCISD calculations. The QCISD without triples reverses the order with the *trans*- barrier now lying ~1–2 kcal/mol below the *cis*- barrier. The inclusion of triples puts the *cis*- barrier lower than the *trans*- barrier, as seen in all of the other PUMP4 and QCISD(T) results. Apparently, the triples play an important role in the details of the relative energetics of these transition states.

It is also interesting to compare the PUMP4/aug-cc-pVTZ barrier height with the QCISD(T)/aug-cc-pVTZ value. The PUMP4 predicts a 1.9 kcal/mol difference between the two barriers, notably larger than the 0.10 kcal/mol difference predicted by QCISD(T). We see the same trend of QCISD(T) narrowing the energy difference between the *cis*- and *trans*- barriers compared to the PUMP4 separation for the 6-311+G(2df,2p) basis. This could attribute to the "often unsatisfactory" convergence of the MP series (Krishnan, Frisch, and Pople 1980).

Figure 3 is an attempt to detect a trend in relative energies for [k] and [l] with respect to the level of correlation correction and basis sets used in the calculations. Admittedly, we cannot state with certainty that the results in any one column of Table 3 are more accurate than another. However, based on our conclusions regarding reaction enthalpies, it will be assumed that the calculations become more accurate as one proceeds from left to right in Figure 3 and in Table 3. An approach to convergence for the barrier heights of [k] and [l] with respect to level of basis set and correlation theory is apparent in Figure 3. The converged value for each is in the range of 5–6 kcal/mol.

Tsunashima et al. (1975) report a pre-exponential factor for Reaction (II) that is smaller than many hydrogen-abstraction reactions and conclude that (II) has a low entropy of activation. They make a rough estimate for the entropy of the activated complex and state that agreement with experiment can be achieved if the complex has a degenerate bending mode of 400 cm^{-1}. (They have assumed a linear structure for [k] or [l] and hence the statement of a "degenerate" bending mode.) They then suggest that this "... indicates a rather tight structure for the activated complex." All three levels of theory used in this work, as well as in our previous study, predict two nonlinear transition states leading to the *cis*- and *trans*-isomers of HSCO. The geometric parameters shown in Figure 1 corresponding to [k] and [l] show the OCS angles as 173° and 171° for the *trans*- and *cis*- barriers, respectively. The HSC angles are 103° and 115° for [k] and [l], respectively. The lowest energy bending modes (from the reference set) have frequencies of 479 cm^{-1} and 415 cm^{-1} for [k] and [l], respectively (Table 4). The UMP2/aug-cc-pVTZ results give 466 cm^{-1} and 396 cm^{-1}, respectively (Table 4). The sizes of the vibrational frequencies of the bound modes of the saddle points support the analysis provided by Tsunashima et al. (1975) of a tight activated complex, although we do not show linear activated complexes that lead to products.

Before we can compare the theoretical energies to the experimental rate measurements, corrections for zero-point energy must be applied. There are no experimental frequencies available for transition states [k] and [l] to use to make these corrections. In addition to the zero-point energy correction, tunneling must be considered. Schatz (1987), in his review of the effect of tunneling on bimolecular collisions, urges the reader to use "extreme caution" when comparing barriers (such as those presented here) to experimentally determined activation energies, due to possibly significant tunneling effects. He lists several studies that show substantial contribution to the rate due to tunneling for hydrogen reactions. He cites specific examples for reduction of activation energy due to tunneling; the reactions cited are H + H_2 and H + HD. Arrhenius fits to the rates between 200 K and 300 K show that the activation energy is lowered by 3.8 kcal/mol and 3.7 kcal/mol for the H + H_2 and H + HD reactions, respectively,

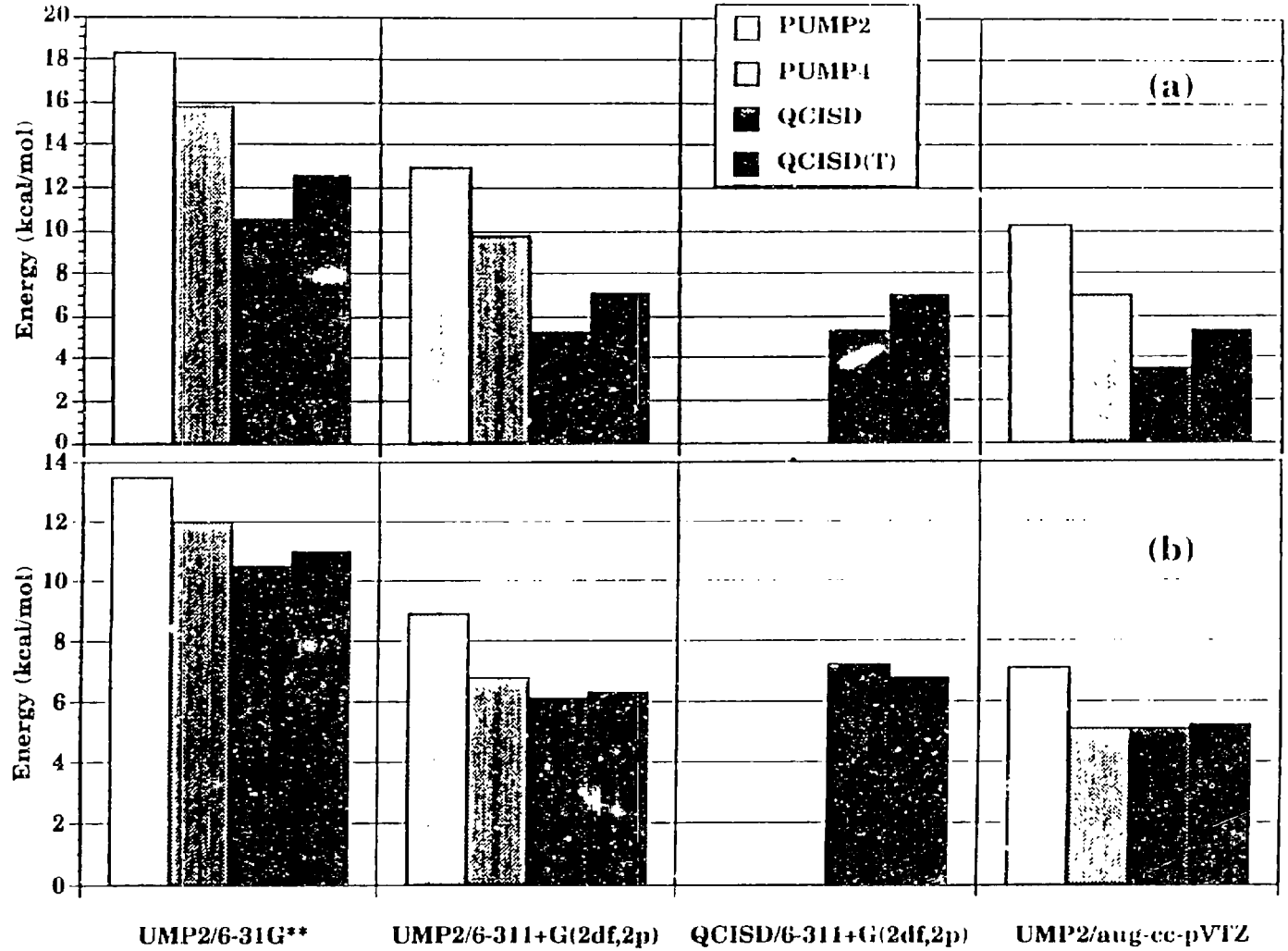

Figure 3. Dependence of the entrance channel barrier heights for Reaction (II) on level of correlation and basis set. (a) *trans*-HSCO entrance channel barrier (structure [k], Figure 1); (b) *cis*-HSCO entrance channel barrier (structure [l], Figure 1). The labeling along the abscissa denotes the level of theory used to calculate the optimized structures. The legend associates the bar type with the correlation level used to refine the energy at that structure.

when tunneling is included. Additionally, Schatz also shows that the pre-exponential factors for these reactions change by orders of magnitude when tunneling is included. It is reasonable to expect that tunneling will contribute to the thermal rate for this reaction. Based on the work reviewed by Schatz (1987), this contribution could be as large as 3–4 kcal/mol. Any further attempt to quantify this contribution, however, is outside the scope of this study.

Kudla, Schatz, and Wagner (1991), in their study of the OH + CO (the isovalent reverse of reactions presented here) considered the decay rate of the four-body HOCO reaction intermediate to H + CO_2. They found, in a tunneling-corrected RRKM calculation, that the rate of decay is very sensitive to character of the saddle point between HOCO and H + CO_2. For example, they showed that tunneling has little effect on the rate (~33% increase) if the barrier has an imaginary frequency of 523*i* cm^{-1}, but a large effect (742% increase) when the frequency is 1,500*i* cm^{-1}. The imaginary frequencies (at the UMP2/aug-cc-pVTZ level) for the saddle points leading to *cis*- and *trans*-HSCO are 1,354*i* cm^{-1} and 723*i* cm^{-1}, respectively. This suggests that tunneling might be significant for *cis*-HSCO formation.

The zero-point energy corrected values for the QCISD(T)//UMP2/aug-cc-pVTZ barriers to formation of *cis*-HSCO and *trans*-HSCO are 5.7 kcal/mol and 8.4 kcal/mol, respectively. The *cis*- barrier, after zero-point energy correction, is within 1.9 kcal/mol of the reported experimental activation energies, without considering tunneling. The zero-point energy corrected value for the *trans*- species indicates that in order to be competitive with the *cis*- species, tunneling must lower the activation energy by ~4.5 kcal/mol. If this system behaves as the analogous H + CO_2 reaction cited by Kudla, Schatz, and Wagner (1991), tunneling would be less for formation of *trans*-HSCO than *cis*-HSCO due to the characterization of the saddle point provided by the imaginary frequencies. This leads to the conclusion that reaction via the formation of *cis*-HSCO is probably the dominant path for thermal reaction. It also suggests that the theoretical results presented here can be considered to be in good agreement with the experimental rate measurements. Even the presumably less accurate reference set energy for the *cis*- entrance barrier (including zero-point energy correction) still falls within 3 kcal/mol of the experimental value, without considering tunneling.

Finally, we attempt to assess the uncertainty in the theoretical results. To do this successfully, one must have reliable experimental numbers. We have chosen (assumed) the critically evaluated reaction enthalpies of Chase et al. (1985), and the experimental activation energy of 3.9 kcal/mol (Tsunashima et al. 1975; Lee, Stief, and Timmons 1977) for Reaction (II) to meet this requirement. The reference set of

calculations gives a reaction enthalpy differing from experiment by 2.6 kcal/mol for Reaction (I) and 3.3 kcal/mol for Reaction (II). The *cis*- entrance barrier (reference set energy, with zero-point correction, no tunneling) is within 3 kcal/mol of the experimental activation energy. Putting error bars on every point on the PES is not possible, but in light of the agreement between theory and what little we know experimentally about [k] and [l], the ±3.3 kcal/mol uncertainty seems a reasonable estimate for most points on the PES.

4. CONCLUSIONS

We have attempted to refine features of the H + OCS potential energy surface from our previous study, using better basis sets and potentially better correlation techniques. In the previous work (Rice, Cartland, and Chabalowski 1993), we located structures at the UMP2/6-31G** level, followed by energy refinements using PUMP4. All structures located in the earlier work were found in this study at the UMP2/6-311+G(2df,2p) level. We found an additional transition state structure corresponding to hydrogen migration from *cis*-HOCS to *cis*-HSCO.

The general features of the PES (structures, relative barriers, and local minima) are qualitatively the same as those in our previous study (Rice, Cartland, and Chabalowski 1993). These features were used to explain the observed product energy distributions for Reactions (I) and (II). The nonstatistical product energy distributions for SH and CO could be explained by the relative sizes of the entrance and exit channel barriers and well depths for the HSCO molecule. Upon crossing the larger entrance channel barrier into a region of the PES corresponding to the HSCO minimum, the molecule has excess energy to overcome the small exit channel barrier, which could easily occur before IVR is complete. The statistical product energy distributions for OH + CS, on the other hand, can be explained in light of the large exit channel barrier leading to OH + CS. The size of the barrier is close to the reaction endothermicity, which must be localized in the reaction coordinate before reaction can proceed. This almost ensures that the molecule will be long-lived, resulting in more complete IVR and statistical product energy distributions. These conclusions remain unchanged, as the relative features of the PES are unchanged: The larger barriers remain large, and the smaller barriers are small. The well depths do not decrease appreciably. The most important differences in the PES are the decreases in the entrance channel barriers leading to *cis*- and *trans*-HSCO. The best uncorrected estimates from this study predict that the *trans*- and *cis*- barriers are almost equal in magnitude. The best calculated theoretical values for the *trans*- and *cis*- barriers, excluding any quantum or dynamic corrections, are 5.3 kcal/mol and 5.2 kcal/mole,

respectively. Upon applying zero-point energy corrections, the energy separation between the two barriers is 2.65 kcal/mol, with the *cis*- barrier being only 1.9 kcal/mol higher in energy than the measured activation energy (~3.9 kcal/mol). Making a reasonable approximation for tunneling and inclusion of the zero-point energy brings the value for the barrier to formation of *cis*-HSCO into good agreement with the experimental measurements. The zero-point energy corrected barrier to formation of *trans*-HSCO, on the other hand, is ~4.5 kcal/mol larger than the experimentally measured activation energy, suggesting that unless tunneling plays a significantly greater role in overcoming the *trans*- entrance barrier than it does for the *cis*- barrier, this pathway will not be competitive with the *cis*- channel for thermal reaction.

Additionally, we have located a previously unreported saddle point between the *cis*-HOCS and *cis*-HSCO species, which confirms the hydrogen-migration route hypothesized by Häusler, Rice, and Wittig (1987). However, the magnitude of the calculated barrier suggests this is not an energetically favored path to formation of SH + CO.

In addition to addressing the thermal rate experiments, we have compared effects on the entrance channel barrier heights and reaction enthalpies from different correlation treatments and basis sets. The calculated reaction enthalpies that agree most closely with experiment are the QCISD(T) calculations using the aug-cc-pVTZ basis. These same calculations provide the lowest entrance channel barriers to reaction.

INTENTIONALLY LEFT BLANK.

5. REFERENCES

Amos, R. D., and J. E. Rice. CADPAC: The Cambridge Analytic Derivatives Package. Cambridge: issue 5.0, 1992.

Andzelm, J., M. Kiobukowski, and E. Radzio-Andzelm. J. Comput. Chem., vol. 5, p. 146, 1984.

Böhmer, E., K. Mikhaylichenko, and C. Wittig. J. Chem. Phys., vol. 99, p. 6545, 1993.

Boys, S. F., and F. Bernardi. Mol Phys., vol. 19, p. 553, 1970.

Chase, M. W., C. A. Davies, J. R. Downey, D. J. Frurip, R. A. McDonald, and A. N. Syverud. "JANAF Thermochemical Tables, Third Edition." J. Phys. Chem. Ref. Data Supplement 1, vol. 14, 1985.

Curtiss, L. A., K. Raghavachari, G. W. Trucks, and J. A. Pople. J. Chem. Phys., vol. 94, p. 7221, 1991.

Davidson, E. R., and D. Feller. Chem. Rev., vol. 86, p. 681, 1986.

Dunning, T. H. J. Chem. Phys., vol. 90, p. 1007, 1989.

Frisch, M. J., G. W. Trucks, M. Head-Gordon, F. M. W. Gill, M. W. Wong, J. B. Foresman, B. G. Johnson, H. B. Schlegel, M. A. Robb, E. S. Replogle, R. Gomperts, J. L. Andres, K. Raghavachari, J. S. Binkley, C. Gonzalez, R. L. Martin, D. J. Fox, D. J. Defrees, J. Baker, J. J. P. Stewart, and J. A. Pople. Gaussian 92. Pittsburgh, PA: Gaussian, Inc., Revision A, 1992.

Gordon, M. S. Chem. Phys. Lett., vol. 76, p. 163, 1980.

Hariharan, P. C., and J. A. Pople. Theor. Chim. Acta, vol. 28, p. 213, 1973.

Häusler, D., J. Rice, and C. Wittig. J. Phys. Chem., vol. 91, p. 5413, 1987.

Hehre, W. J., R. Ditchfield, and J. A. Pople. J. Phys. Chem., vol. 56, p. 2257, 1972.

Herzberg, G. Infrared and Raman Spectra of Polyatomic Molecules. Princeton: Van Nostrand, 1945.

Huber, K. P., and G. Herzberg. Molecular Spectra and Molecular Structure. IV. Constants of Diatomic Molecules. New York: Van Nostrand Reinhold, 1979.

Kendall, R. A., T. H. Dunning, and R. J. Harrison. J. Chem. Phys., vol. 96, p. 6796, 1992.

Krishnan, R., and J. A. Pople. Int. J. Quant. Chem., vol. 14, p. 91, 1978.

Krishnan, R., J. S. Binkley, R. Seeger, and J. A. Pople. J. Chem. Phys., vol. 72, p. 650, 1980.

Krishnan, R., M. J. Frisch, and J. A. Pople. J. Chem. Phys., vol. 72, p 4244, 1980.

Kudla, K., G. C. Schatz, and A. F. Wagner. J. Chem. Phys., vol. 95, p. 1635, 1991.

Lee, J. H., L. J. Stief, and R. B. Timmons. J. Chem. Phys., vol. 67, p. 1705, 1977.

McLean, A. D., and G. S. Chandler. J. Chem. Phys., vol. 72, p. 5639, 1980.

Møller, C., and M. S. Plesset. Phys. Rev., vol. 46, p. 618, 1934.

Nickolaisen, S. L. Ph.D. dissertation, University of Southern California, 1991.

Nickolaisen, S. L., and H. E. Cartland. J. Chem. Phys., vol. 99, p 1145, 1993.

Oldershaw, G. A. and A. Smith. J. Chem. Soc. Faraday Trans. I, vol. 74, p. 1687, 1978.

Oldershaw, G. A., and D. A. Porter. J. Chem. Soc. Faraday Trans. I, vol. 68, p. 709, 1972.

Pople, J. A., M. Head-Gordon, and K. Raghavachari. J. Chem. Phys., vol. 87, p. 5968, 1987.

Pople, J. A., M. Head-Gordon, D. J. Fox, K. Raghavachari, and L. A. Curtiss. J. Chem. Phys., vol. 90, p. 5622, 1989.

Rice, B. M., H. E. Cartland, and C. F. Chabalowski. Chem. Phys. Lett., vol. 211, p. 283, 1993.

Schatz, G. C. Chem. Rev., vol. 87, p. 81, 1987.

Schwenke, D. W., and D. G. Truhlar. J. Chem. Phys., vol. 82, p. 2418, 1985.

Schwenke, D. W., and D. G. Truhlar. J. Chem. Phys., vol. 84, p. 4113, 1986.

Simandiras, E. D., R. D. Amos, N. C. Handy, T. J. Lee, J. E. Rice, R. B. Remington, and H. F. Schaefer. J. Am. Chem. Soc., vol. 110, p. 1388, 1988.

Tsunashima, S, T. Yokota, I. Safarik, H. E. Gunning, and O. P. Strausz. J. Phys. Chem., vol. 79, p. 775, 1975.

Wagman, D. D., W. H. Evans, V. B. Parker, R. H. Schumm, I. Halow, S. M. Bailey, K. L. Churney, and R. L. Nuttall. "The NBS Tables of Chemical and Thermodynamic Properties." J. Phys. Chem. Ref. Data Supplement 2, vol. 11, 1982.

Woon, D. E., and T. H. Dunning. J. Chem. Phys., vol. 98, p. 1358, 1993.

NO. OF COPIES	ORGANIZATION
2	ADMINISTRATOR DEFENSE TECHNICAL INFO CENTER ATTN: DTIC-DDA CAMERON STATION ALEXANDRIA VA 22304-6145
1	COMMANDER US ARMY MATERIEL COMMAND ATTN: AMCAM 5001 EISENHOWER AVE ALEXANDRIA VA 22333-0001
1	DIRECTOR US ARMY RESEARCH LABORATORY ATTN: AMSRL-OP-SD-TA/ RECORDS MANAGEMENT 2800 POWDER MILL RD ADELPHI MD 20783-1145
3	DIRECTOR US ARMY RESEARCH LABORATORY ATTN: AMSRL-OP-SD-TL/ TECHNICAL LIBRARY 2800 POWDER MILL RD ADELPHI MD 20783-1145
1	DIRECTOR US ARMY RESEARCH LABORATORY ATTN: AMSRL-OP-SD-TP/ TECH PUBLISHING BRANCH 2800 POWDER MILL RD ADELPHI MD 20783-1145
2	COMMANDER US ARMY ARDEC ATTN: SMCAR-TDC PICATINNY ARSENAL NJ 07806-5000
1	DIRECTOR BENET LABORATORIES ATTN: SMCAR-CCB-TL WATERVLIET NY 12189-4050
1	DIRECTOR US ARMY ADVANCED SYSTEMS RESEARCH AND ANALYSIS OFFICE ATTN: AMSAT-R-NR/MS 219-1 AMES RESEARCH CENTER MOFFETT FIELD CA 94035-1000

NO. OF COPIES	ORGANIZATION
1	COMMANDER US ARMY MISSILE COMMAND ATTN: AMSMI-RD-CS-R (DOC) REDSTONE ARSENAL AL 35898-5010
1	COMMANDER US ARMY TANK-AUTOMOTIVE COMMAND ATTN: AMSTA-JSK (ARMOR ENG BR) WARREN MI 48397-5000
1	DIRECTOR US ARMY TRADOC ANALYSIS COMMAND ATTN: ATRC-WSR WSMR NM 88002-5502
1	COMMANDANT US ARMY INFANTRY SCHOOL ATTN: ATSH-WCB-O FORT BENNING GA 31905-5000
	ABERDEEN PROVING GROUND
2	DIR, USAMSAA ATTN: AMXSY-D AMXSY-MP/H COHEN
1	CDR, USATECOM ATTN: AMSTE-TC
1	DIR, USAERDEC ATTN: SCBRD-RT
1	CDR, USACBDCOM ATTN: AMSCB-CII
1	DIR, USARL ATTN: AMSRL-SL-I
5	DIR, USARL ATTN: AMSRL-OP-AP-L

NO. OF COPIES	ORGANIZATION
1	HQDA (SARD-TR/MS K KOMINOS) WASH DC 20310-0103
1	HQDA (SARD-TR/DR R CHAIT) WASH DC 20310-0103

USER EVALUATION SHEET/CHANGE OF ADDRESS

This Laboratory undertakes a continuing effort to improve the quality of the reports it publishes. Your comments/answers to the items/questions below will aid us in our efforts.

1. ARL Report Number ARL-TR-629 Date of Report November 1994

2. Date Report Received _____

3. Does this report satisfy a need? (Comment on purpose, related project, or other area of interest for which the report will be used.) _____

4. Specifically, how is the report being used? (Information source, design data, procedure, source of ideas, etc.) _____

5. Has the information in this report led to any quantitative savings as far as man-hours or dollars saved, operating costs avoided, or efficiencies achieved, etc? If so, please elaborate. _____

6. General Comments. What do you think should be changed to improve future reports? (Indicate changes to organization, technical content, format, etc.) _____

CURRENT ADDRESS

_____
Organization

_____
Name

_____
Street or P.O. Box No.

_____
City, State, Zip Code

7. If indicating a Change of Address or Address Correction, please provide the Current or Correct address above and the Old or Incorrect address below.

OLD ADDRESS

_____
Organization

_____
Name

_____
Street or P.O. Box No.

_____
City, State, Zip Code

(Remove this sheet, fold as indicated, tape closed, and mail.)
(DO NOT STAPLE)